buildings

MDPI

Article

Numerical Simulation of the Performance of Self-Healing Concrete in Beam Elements

Khalid Alkhuzai [1], Luigi Di Sarno [2], Abdullah Haredy [3,*], Raed Alahmadi [1] and Danah Albuhairi [2]

[1] Department of Civil Engineering, Faculty of Engineering, Albaha University, Albaha 65731, Saudi Arabia
[2] School of Engineering, University of Liverpool, Liverpool L69 3GH, UK
[3] Department of Architecture, Faculty of Engineering, Albaha University, Albaha 65731, Saudi Arabia
* Correspondence: aaharedy@bu.edu.sa

Abstract: The formation of cracks in concrete structures occurs due to a multitude of causes ranging from shrinkage to external loading and environmental exposure. This phenomenon can significantly affect the lifecycle of concrete structures. Self-healing concrete (SHC) is considered a promoted innovation capable of overcoming this inevitable occurrence. In accordance with current SHC development processes, this paper utilizes the numerical simulation approach to test the performance of reinforced SHC beam specimens modeled using the commercial software ABAQUS 6.14 (Vélizy-Villacoublay, France). This paper aims to contribute to the scarce literature on SHC models by utilizing the overlooked dicyclopentadiene (DCPD) agent and ambiguous variability of crystalline admixtures. The SHC is introduced to the beam models at various depths and analyzed using load against displacement curves compared with a reference model of ordinary concrete. The effects of SHC on the mechanical properties of structural elements were determined. The results show a distinct improvement of the load-carrying capacity of SHC beams, indicating an efficient contribution of SHC in structural applications.

Keywords: self-healing concrete; finite element modeling; structural resilience; sustainability

check for updates

Citation: Alkhuzai, K.; Di Sarno, L.; Haredy, A.; Alahmadi, R.; Albuhairi, D. Numerical Simulation of the Performance of Self-Healing Concrete in Beam Elements. *Buildings* **2023**, *13*, 809. https://doi.org/10.3390/buildings13030809

Academic Editors: Cesare Oliviero Rossi, Pietro Calandra, Paolino Caputo, Bagdat Teltayev, Valeria Loise and Michele Porto

Received: 14 November 2022
Revised: 4 February 2023
Accepted: 7 February 2023
Published: 19 March 2023

Copyright: © 2023 by the authors. Licensee MDPI, Basel, Switzerland. This article is an open access article distributed under the terms and conditions of the Creative Commons Attribution (CC BY) license (https://creativecommons.org/licenses/by/4.0/).

1. Introduction

As the most widely consumed construction material, concrete possesses a high flexibility for various applications. In a typical steel reinforced concrete structure, crack formation threatens the corrosion of reinforcement, leading to a compromised durability. As such, costly and inconvenient maintenance and manual crack repair become a requirement. The application of self-healing concrete (SHC) with autonomous crack repair and property recovery promises substantial development in concrete constructions.

The SHC technology has a significant trend regarding environmental and economic sustainability for an improved lifecycle [1–5]. Moreover, SHC's healing processes is fairly durable due to the long life of embedded systems [1,6], promising longer structural service life. In contrast, alternative treatments, such as applying chemicals (e.g., epoxy resins, waxes, and acrylic) and polymers are prone to weathering, sustainability issues, weak bonding with concrete, and degradation with age [7]. SHC can be applied as a building facade protection and refurbishment, cement mortar to create a self-healing product, fostering road construction and limestone structure (e.g., historic structures) [8–10]. In large-scale applications, SHC is suitable for structures exposed to wet environments, such as marine structures susceptible to reinforcement corrosion. Additionally, tunnels, underground structures, infrastructures, and bridges are also suitable applications of self-healing concrete; other possible applications include tunnel-lining, structural basement walls, highway bridges, concrete floors, and marine structures [11].

SHC mechanisms are established across two main strategies: autogenous and autonomous healing using either chemical (i.e., mineral or expansive admixtures, etc.), or

biological components (i.e., microorganisms such as bacteria or fungi, etc.) [12]. The autogenous healing strategy relies on prolonging the natural chemical processes of maturing concrete in which hydration may contribute to crack closure. However, this is limited to smaller crack widths due to finite hydration phases and has a high reliance on environmental conditions. Autonomous healing strategies often make use of immobilization techniques where a healing agent is kept dormant mainly within an encapsulation system, or a vascular network system. The latter strategy has gained popularity due to its ability to challenge the shortcomings of natural healing in addressing larger crack widths over prolonged periods.

The current direction of research promises to highly regard the use of computer modeling to achieve material optimization [13–16]. In summary, the earlier instances of simulating SHC performance has involved the autogenous healing where the delayed hydration of cement was the target of assessment [17]. More recently, numerical simulations are targeting SHC performance at the structural element level [18].

1.1. Research Gaps and Future Perspective

There exist several research areas aimed towards SHC progression for use in construction. However, the gap in research of SHC lies in the lack of conclusive field studies and limited reports regarding the feasibility of SHC in its use for structural applications. Hence, the standardization of SHC in construction is unlikely to be achieved solely through more laboratory and field studies, hinting at the need for alternative testing methods such as computer modeling techniques. This approach attains the design by testing standard while productively contributing to the lack of understanding involving the chosen healing systems (i.e.,: crystalline admixture and dicyclopentadiene). It is anticipated that this work will shed light on an important aspect of SHC testing and development for construction, with specific regard to enhancing the attention of research on the several technical deficiencies found in employing numerical simulation of a relatively unexplored model. Furthermore, recent numerical studies have highlighted the need for developing three-dimensional models of SHC [14]. The framework basis of this study therefore includes:

1. Finite element study carried out with an advanced and reliable numerical simulation platform;
2. Constitutive models, including details of the material properties of ordinary concrete, the reinforcement, and the SHC, in addition to the model configuration showing elements and meshing types;
3. Modeling the reference beam (reinforced concrete beam);
4. Validating the deflection obtained from simulation with the theoretical formula;
5. Modeling the SHC beams.

The outcomes of the present numerical study show that the use of SHC may significantly improve the structural performance of ordinary reinforced beams, as illustrated hereafter.

1.2. Previous Work on Mechanical Properties of SHC

The lack of standards in preparing and testing SHC are further enhanced by the wide variations of healing systems. As such, this paper aims to minimize the mystified applications of SHC in construction by employing healing agents which have shown promising practicality yet remain ambiguous in performance. This paper aims to address this gap by investigating the existing technical literature of commonly and controversially reported self-healing systems to observe the implications of SHC on a structural beam element. Two parameters are adopted from selected literature for this study, namely the modulus of elasticity and the tensile strength of the given SHC system to investigate the structural performance of selected healing systems.

Self-healing material that is amongst the most convenient to implement is the crystalline admixture (CA). However, CA is widely commercialized with varying compositions used across research, hindering validation and progress in understanding its self-healing

potential [19]. The CA may be introduced into the concrete without strategic techniques such that it can be mixed without compromising its composition [20]. This paper uses the tensile properties reported in an experiment conducted to study the mechanical properties of fiber-reinforced SHC samples containing 1.1% of the CA, and samples were pre-cracked at the age of 2 and 28 days before curing [21]. Following healing at 28 days, the water-cured samples have shown the highest mechanical properties where the splitting tensile strength had an increase of 2.88% and the compressive strength was increased by 13.98%. In a study using numerical modeling of SHC containing CA, there was a reported improvement in the recovery of the load-bearing capacity of specimens after cracking [22].

Another seemingly underreported yet promising healing agent is dicyclopentadiene (DCPD) [23]. In an experimental study investigating the properties of DCPD SHC, two healing agents were used and tested, namely, DCPD and sodium silicate (SS) [24]. Concrete cylinder specimens were prepared using a standard ready-mix concrete with a water/cement ratio of 0.5 and a nominal compressive strength of 28 MPa. The healing activity was tested with loading and unloading cycles; the specimens were then left to cure for 48 h. The modulus of elasticity was tested conforming to ASTM C 469 with the variation of applying 70% of the peak strength, followed by the comparison of the concrete with and without self-healing microcapsules before and after a 1-week healing period. In terms of practicality, sample preparation was more convenient with the SS microcapsules prepared at a pH of 3.1 and added to the mixing water at a content of 5% by weight of cement. However, the modulus of elasticity was found to be higher in samples containing DCPD at a content of 0.25% by weight of cement. The Young's modulus of the concrete with DCPD was 33.68 GPa and 40.54 GPa before and after healing, respectively; whereas the SS specimens reported 32.88 GPa and 34.80 GPa before and after healing, respectively.

2. Materials and Methods

The commercial software Abaqus 6.14 (Dassault Systemes, 2014) [25] is used for the analysis of the structural engineering performance of reinforced beam elements containing SHC. A total of seven models with identical dimensions (0.3 × 0.6 cross-section and 6 m length) have been analyzed to study the influence of SHC on a structural beam. The control model is a reinforced concrete (RC) beam, created as a reference to capture the typical behavior of a structural beam member under distributed loads. The other six models are self-healing concrete beams treated to various depths, ranging from 100 mm past the lower bound to the full depth of the beam (600 mm) as shown in Figure 1.

The SHC has a layered design, which functions as a single composite component within the normal concrete. Additionally, the steel reinforcement bars are 4Ø16 at the tension zone of the beam and 2Ø16 at the compression zone, whereas the shear links are 42Ø8 distributed along the beam, with spacings of 145 mm. The design of the reference beams is based on the provisions implemented in Eurocode 2 [26] and ACI (1995) [27].

A significant number of constitutive models built to describe the mechanical behavior of RC members exist, however, there are no specific constitutive models available of the finite element (FE) solutions for the structural analysis of SHC members. The concrete damaged plasticity (CDP) model used is based on the model proposed by Lubliner et al. [28] and Lee and Fenves [29], with the concrete smeared cracking (CSC) assumption adopted. This model assumes a damaged isotropic elasticity, combined with isotropic tensile and compressive plasticity to reflect concrete's inelastic behavior. This model is generally accepted to be reliable and as it can efficiently detect the formation and propagation of cracks to accurately capture the permanent damage occurring during the fracturing process [30]. As such, the CDP model is a commonly used method across different simulation software in analyzing RC structures [31,32].

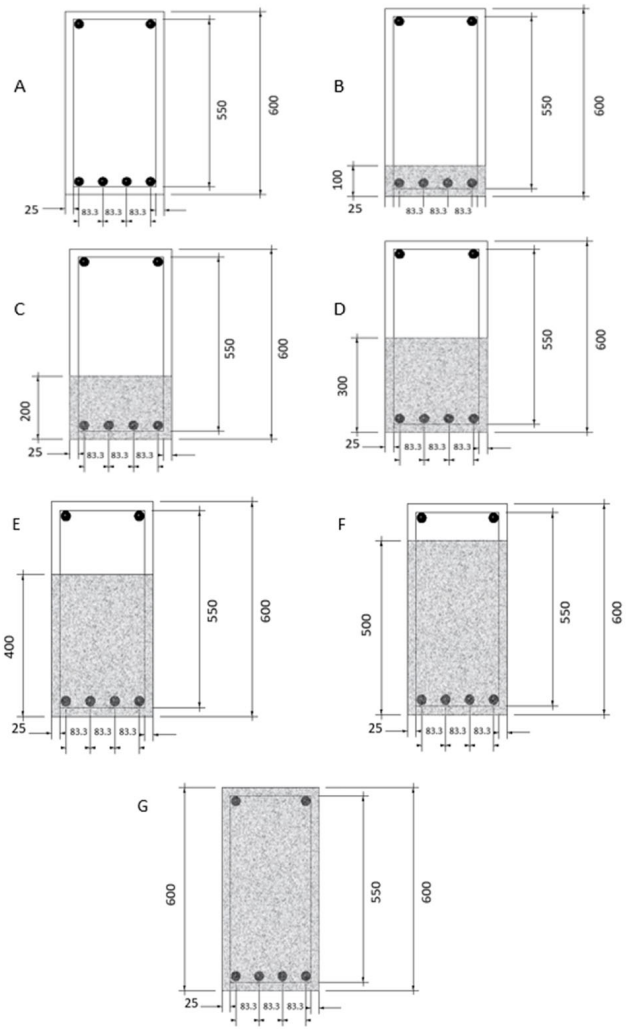

Figure 1. Designed cross-sections. (**A**) Reference beam. (**B**) Addition of SHC at 100 mm. (**C**) Addition of SHC at 200 mm. (**D**) Addition of SHC at 300 mm. (**E**) Addition of SHC at 400 mm. (**F**) Addition of SHC at 500 m. (**G**) Full SHC section.

2.1. Constitutive Models

2.1.1. Material Properties of Concrete and Steel Reinforcement

The uniaxial compressive stress–strain relationship in the present CDP model is considered as an elasticity that is perfectly applicable to both concrete and steel. The CDP model requires that the elastic behavior of the material be isotropic and linear, hence, the beams are modeled as such. The model assumes two main failure mechanisms, namely the tensile cracking and compressive degradation of the concrete. The CSC assumption represents the discontinuous macrocrack brittle behavior where cracks are accounted on the basis of their effect on the stress and material stiffness. The use of such model is to avoid convergence problems for the FEM simulations carried out with Abaqus, as it requires high computational capacity.

Microcracking in the concrete is represented by the increase in the values of hardening variables. The hardening variables characterize damaged states in tensile cracking and compressive crushing independently. These variables govern the yield surface evolution and elastic stiffness degradation in relation to the dissipated fracture energy generating microcracks and is expressed as:

$$\dot{\tilde{\varepsilon}}^{pl} = h\left(\bar{\sigma}\,,\,\tilde{\varepsilon}^{pl}\right)\,.\,\dot{\varepsilon}^{pl},$$

where $\dot{\varepsilon}^{pl}$ is the plastic part of the strain rate, and $h\left(\overline{\sigma}, \widetilde{\varepsilon}^{pl}\right)$ is the stiffness degradation variable used to calculate the Cauchy stress. The Cauchy stress is related to the effective stress through the stiffness degradation relation governing the effective stress:

$$\sigma = (1 - d)\overline{\sigma}$$

where σ is the stress, $(1 - d)$ is the ratio of the effective load-bearing area, and $\overline{\sigma}$ is the effective stress. Where no damage exists, the effective stress is equivalent to the Cauchy stress. However, the effective stress is more representative than the Cauchy stress in the event of damage occurrence such that it portrays the effective stress area resisting loads. As such, damage related to the failure mechanisms of the concrete (cracking and crushing) manifest as reductions in the elastic stiffness, hence the basic assumption of linear elasticity.

Plastic flow is governed by a flow potential G according to the flow rule:

$$\dot{\varepsilon}^{pl} = \dot{\lambda}\frac{\partial G(\overline{\sigma})}{\partial \overline{\sigma}}$$

where $\dot{\varepsilon}^{pl}$ is the plastic part of the total strain rate, $\dot{\lambda}$ is the nonnegative plastic multiplier, and $\dot{\lambda}$ and F obey the Kuhn–Tucker conditions: $\dot{\lambda}F = 0;\ \dot{\lambda} \geq 0; F \leq 0$.

As such, the elastic–plastic damage response is portrayed in terms of effective stress and hardening variables with the constitutive relations summarized as:

$$\sigma = D_0^{el} : \left(\varepsilon - \varepsilon^{pl}\right)\ \epsilon\ \left\{\overline{\sigma} | F\left(\overline{\sigma}, \widetilde{\varepsilon}^{pl}\right) \leq 0\right\},$$

where D_0^{el} is the undamaged elastic stiffness, ε is the strain rate, ε^{pl} is the plastic strain rate, and $F\left(\overline{\sigma}, \widetilde{\varepsilon}^{pl}\right)$ is the yield function capped as an inviscid model.

Since the grade of the concrete used is C25/30, the material parameters are calculated according to EN1992-1-1. The mean compressive strength is calculated using Equation (1):

$$f_{cm} = 8 + f_{ck} \tag{1}$$

where f_{cm} (MPa) is the mean compressive strength and f_{ck} (MPa) relates to characteristic compressive cylinder strength of concrete at 28 days.

The longitudinal modulus of elasticity of the concrete can be calculated using the relations available in Equation (2):

$$E_{cm} = 22,000 \times \left(\frac{f_{cm}}{10}\right)^{0.3} \tag{2}$$

where E_{cm} (GPa) is the longitudinal modulus of elasticity and f_{cm} (MPa) is the mean compressive strength of concrete.

The tensile strength of concrete under uniaxial stress is difficult to assess, and the results are very scattered. Therefore, it should be determined according to EN1992-1-1, as in Equation (3):

$$f_{ctm} = 0.30 f_{ck}{}^{\left(\frac{2}{3}\right)} \tag{3}$$

where f_{ctm} (MPa) is the mean value of axial tensile strength of concrete and f_{ck} is the characteristic compressive cylinder strength of concrete at 28 days.

The material properties assigned for concrete are shown in Table 1 and steel properties are shown in Table 2.

Table 1. Material properties of ordinary concrete.

Concrete	C25/30
f_{ck} (MPa)	25
f_{cm} (MPa)	33
E_c (MPa)	31,476
f_{ctm} (MPa)	2.56
v	0.2

Table 2. Material properties of steel.

Steel	B500C
fs (MPa)	500
E_c (MPa)	200,000
v	0.3

Moreover, the five input parameters of the plasticity part of the CDP model are varied within a specified range as shown in Table 3. These parameters are considered default values [32].

Table 3. Plasticity parameters.

Ψ (Dilatation Angle)	e (Eccentricity)	(fb0/fc0)	Kc	Viscosity
36°	0.1	1.16	0.667	0

The actual transition seen in the experiments of the technical literature (after which the specimens are kept for healing) is disregarded such that only the healed properties are studied in reflection of the degree of self-healing. The compressive behavior of the concrete is assumed to be the same as that of ordinary concrete, with a mean compressive strength of 33 MPa. The tensile strength is taken from another experiment in which the CA was used [21]. The elastic modulus of the healed SHC is adopted from an experiment in which the healing agent DCPD was used [24]. The healed material properties of SHC are shown in Table 4.

Table 4. Material properties of SHC.

Concrete	C25/30
f_{ck} healed (MPa)	25
E healed (MPa)	40,540
f_{ctm} healed (MPa)	4
v	0.2
Density, ρ	2.5×10^{-9}

2.1.2. Numerical Model for the Structural Analyses

The three-dimensional 8-node first-order continuum elements (C3D8R-Bricks) are used for reference concrete beams, SHC beams, and bearing steel plates. The other primary components in this analysis are the longitudinal reinforcements modeled as three-dimensional truss elements 2-node linear (T3D2). The T3D2 truss is used to model the reinforcing bars and links in the FE models of all beam specimens. To derive accurate results from the FE model, all the components were allocated a uniform mesh size of 30 to ensure that the same nodes are shared. The 8-node linear brick element is the mesh element type used for modeling concrete, SHC, and bearing plates, with three translation degrees of freedom at each node (C3D8R). The refined mesh discretization included 40,000 shells along with 1200 truss finite elements to accurately simulate the response of concrete and steel reinforcement. Perfect bond was assumed at the interface of steel and concrete.

2.2. Reference Beam Modeling

The reference beam serves as a benchmark comparing the structural performance of a conventional RC beam with SHC models. This assumption is fundamental to perform comparative analyses, due to lack of adequate experimental tests for model calibration and validation. Four parts form the beam models: concrete, steel rebars, steel stirrups, and steel-bearing plates. Moreover, the beam is subjected to excessive loads as a uniformly distributed load (UDL), along the full length of the beam with the applied load of 500 kN, which is equivalent to the UDL of 83.3 kN/m. This is to allow the beam to enter the plastic zone.

The UDL load is converted to point load as shown in the pressure equation resulting in 0.27 MPa applied with the step type of Static, General. The analysis case is demonstrated in Figure 2:

$$\text{Pressure} = \frac{500 \times 1000}{6000 \times 300} = 0.27 \text{ MPa}$$

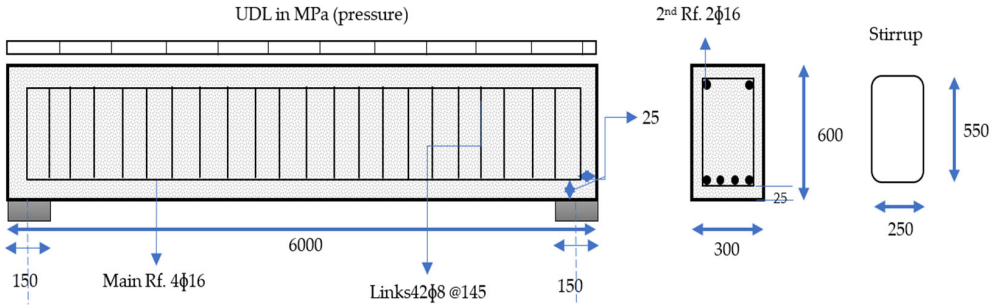

Figure 2. Schematic view of the modeled beam. Note: units in mm.

To establish the boundary conditions, two reference points (RP1 and RP2) are identified immediately below the support. Both points display a "Coupling" interaction with the central element of the bottom face of the support and are assigned as pinned supports. Restricting the central element of the support with the reference point avoids any distortion of the steel plates, such that the support can rotate as one component. Additionally, the reason for creating the reference points is to measure the reaction forces in the supports' bottom face's central element, and then to calculate the total loads on the beam as in Figure 3. Moreover, the upper face of the support interacts with the bottom face of the beam via a "Tie" interaction. Furthermore, the embedded element option is used to connect the reinforcing elements to the concrete element, the steel reinforcement is used as the embedded element, and the concrete is designated as the host.

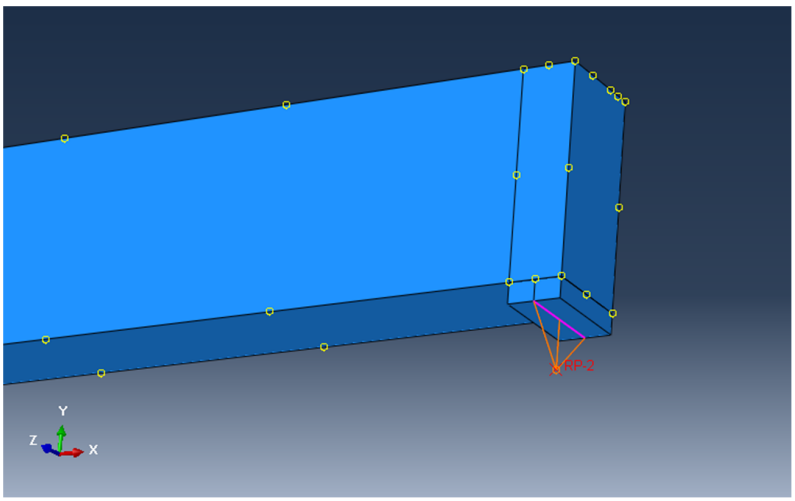

Figure 3. Support interaction with reference points.

2.3. Validation of the Abaqus model through Comparisons with Theoretical Formulations

The model of the RC beam is defined as isotropic and linear for the elastic behavior of the concrete and steel, which can be defined only by the modulus of elasticity and Poisson's ratio. This is because the theoretical formula does not account for plastic deformation. In assessing the percentage difference of deflection attained in using Abaqus, an error percentage of approximately 3% was found where the analytical deflection was 7.24 mm, and theoretical was 7.47 mm as shown in Equation (4):

$$\delta = \frac{5\,\omega\,l^4}{384\,EI} = \frac{5 \times 33.3 \times 5850^4}{384 \times 31476 \times 5.4 \times 10^9} = 7.47 \text{ mm} \quad (4)$$

where δ (mm) is the deflection, ω is the distributed loads, L is the effective span, E is the elastic modulus, and I is the second moment of the area.

2.4. SHC Beam Modeling

In modeling SHC beams, the self-healing component is added as a layer that can work homogeneously with the ordinary concrete. Using the partition tool in Abaqus, we can cut the ordinary concrete and assign the cut part a self-healing material. The mesh, step, and interaction used in the reference beam are also utilized in the SHC models. In partial SHC models, the bottom section of the reference beam is replaced with SHC. Furthermore, the loading cycles and parameters of the SHC models are the same as those of the reference beam, but the applied load is increased to 1000 kN, equivalent to a UDL 166.6 kN/m. This is utilized to account for the increased bearing capacity of the SHC beams and to ensure that plasticity is reached. Furthermore, the analysis is terminated upon reaching the reference beam's peak deflection of 48 mm, by which 60% of the applied load was reached. Plastic deformation also occurred for all SHC specimens. However, the loads were reduced sequentially to cope with the computer capacity and reduce the analysis time.

3. Results

The three main points of relevance for structural behavior observations of the simulation results are characterized at three sections, namely, critical yield, cracking, and ultimate points as shown in Table 5. A representation of the load against deflection curves is shown in Figure 4. The yield point signifies the elastic deformation's limit in which plastic deflection follows to indicate the stiffness of the beam. The latter points are considered in order to assess the behavior of the beams under excessive loads such that the cracking point occurs around significant increases in shear stresses that induce cracks, and the ultimate point is taken as the maximum load-bearing capacity of the beam by which failure is met.

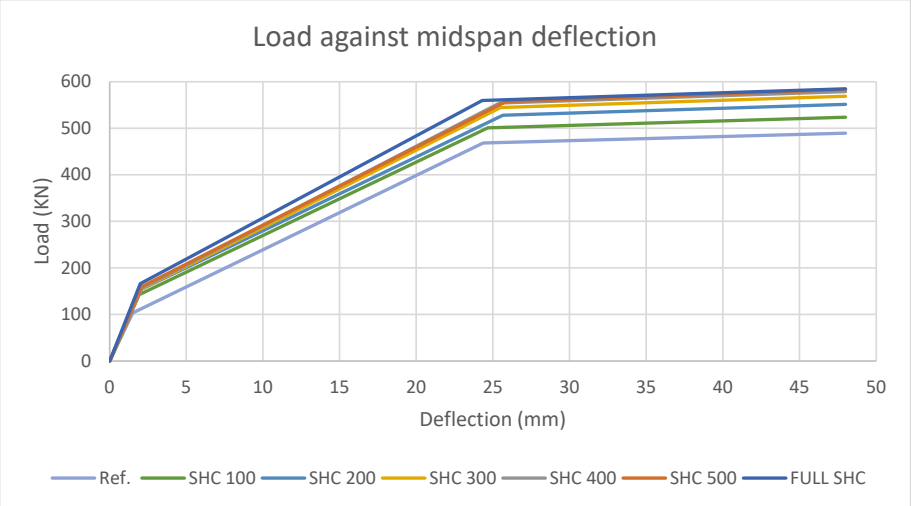

Figure 4. Load against displacement curves of beam models.

Table 5. Beam model deflection and load results at three critical points, and the increase in percentage with respect to the reference model.

	Yield Point		Cracking Point		Max Point	
Model	**Deflection (mm)**	**Load (kN)**	**Deflection (mm)**	**Load (kN)**	**Deflection (mm)**	**Load (kN)**
Ref.	1.505	103.081	24.362	468.285	48.000	489.387
SHC100	1.902	141.949	24.667	500.776	48.000	523.600
SHC200	2.087	154.240	25.654	527.928	48.000	551.278
SHC300	2.070	154.399	25.504	544.401	48.000	568.725
SHC400	2.086	155.897	25.448	554.187	48.000	578.893
SHC500	2.067	159.036	25.842	557.020	48.000	583.322
Full SHC	2.000	166.109	24.308	559.441	48.000	584.741
	Increase in Overstrength (%)		**Increase in Overstrength (%)**		**Increase in Overstrength (%)**	
SHC100	32		7		7	
SHC200	40		13		12	
SHC300	40		12		15	
SHC400	41		17		17	
SHC500	43		17		18	
Full SHC	47		18		18	

4. Discussion

In the reference model, the beam remained in the elastic zone with loads up to 200 kN. The beam yielded at a load of 103 kN, with a maximum deflection of 1.5 mm at the midspan, whereas at the ultimate point, the load was 489 kN, with a deflection of 48.5 mm. Moreover, the beam cracked at a load of 468 kN, with a deflection of 24.3 mm. The yield strength was the property of the beams that showed the most significant improvement with SHC models. It is evident that the load-carrying capacity of SHC beams increased with the increase in SHC depth. Additionally, the midspan deflection was only 0.5 mm higher in the full SHC beam, with an approximate doubling of the yield strength at 46%. However, the increased load-bearing capacity of the beams could indicate positive healing capacity at smaller loads. In agreement with the experimental study adopted for CA, load-carrying capacity has also been improved in incorporating CA. This has been attributed to the formation of hydration products enhancing strain capacity. On the same note, the adopted study using DCPD has also recorded an improvement in the modulus of elasticity in using the healing agent.

Regarding cracking and ultimate strength, all SHC beams exhibited similar behavior, but with minor differences. The reference beam displayed cracks at a load of 468 kN, and deflected up to 24.4 mm. In contrast, the partial SHC models had higher deflections withstand greater loads before cracks formed. However, the deflection of the full SHC beam showed a displacement identical to the reference beam at the cracking point, but it had a higher load capacity. This may be an indication of increased stiffness against tensile stresses in the full SHC beam.

The most notable results of strength increase were found in the yielding strengths of the beams, indicating a possibility for improved concrete elastic behavior with SHC addition. This was also indicated in a study where fibers were added into the SHC mixture to prevent cracks from branching [33], an indication that SHC beams may also benefit structurally from modifications restricting crack propagation. The overall trend of increased displacements could be reasoned with increased loading capacity, however, the partial SHC models lie mostly within the beam's tension zone, hence it can be inferred that the healing system contributes to the overall stiffness. In a study of bacterial self-healing RC beams, higher deflection displacements and higher loads were sustained parallel to increased widths of cracks [34]. This may indicate that at the macroscale, self-healing systems contribute to the elastic behavior of concrete. This occurrence has also been seen in other self-healing concrete systems where larger crack widths are measured in parallel with improved compressive strength values with an alternative sample found healing

larger widths and reporting compromised values [35]. As such, it may be inferred that in practical applications, the efficiency of a healing system is not to be solely measured according to its capacity to restrict cracking. Future investigations may attempt to quantify this phenomenon to understand the influence of higher deflections found in SHC structural members by deriving an expression for stiffness as a function of crack width.

The two healing agents used may be assumed suitable systems to interplay due to the controlled mechanism found in CA and DCPD such that they are not susceptible to premature activation [23,36] and therefore, the degree of spontaneous interplay may be deemed minimal. This is supported by the improved mechanical properties found in using the SHC beam models in comparison with the reference beam lacking these healing agents. Moreover, the general trend of improved properties agrees with the performance reported in the experimental studies adopted. As no studies exist implementing the two healing agents, the practical manifestation of the combined action of DCPD and CA must be experimented for durability properties in recognition of realistic environmental conditions. The validation of the numerical study with an equivalent experiment can enhance confidence in the promising mechanical performance reported, ultimately promoting the use of the ambiguous healing systems.

5. Conclusions

In this study, six models of SHC and one reference model were built using finite element methods (Abaqus software). The SHC beams were modeled as layers, each layer introduced at a certain depth. Additionally, the reference beam was modeled with material properties similar to an ordinary concrete's grade C25/30. Since no large-scale SHC simulation studies have previously been carried out, the mechanical properties of the healed concrete from existing literature were adopted in this study, namely the Young's modulus and tensile strength. Moreover, the concrete's Young's modulus is based on that of healed specimens from experiments in which DCPD was used as a healing agent, and the tensile strength where CA was used. Therefore, the presented results reflect the activation of the self-healing process, and they show that the self-healing material produced higher strength than the reference concrete.

The purpose of this numerical analysis was to study the behavior of an RC beam with and without SHC. Therefore, a comparison between the reference beam and SHC beams was conducted using the mean of the load versus deflection curve. The beams were compared at three points (i.e., yield, cracking, and ultimate points) that reflect the practical performance of each structural beam. According to the simulation results, the following conclusions are drawn:

1. The addition of SHC improved the overall performance of the structural beam;
2. Most significant improvements in the SHC models were achieved in yield strength when lower loads were considered;
3. The small cracks that formed at lower loads seemed to be healed, since the increases in overstrength at these loads were significant (as much as 47% higher than the original strength);
4. There was good indication of the effectiveness of the SHC at excessive loads, such as cracking and ultimate loads;
5. The maximum strength of the SHC beams was higher than the reference beam, with an increase in overstrength of only 18% compared to the original.

6. Further Research

In addition to the undertaken numerical simulation tests, SHC specimens could be tested for compression and flexural strengths to determine compression resistance, tensile strength (indirectly), and Young's modulus. Moreover, an analytical study as such may benefit from verifications with 3D computed tomography scan [14]. Investigations with microscopic analysis of structural elements of SHC could also be conducted to visualize the chemical aspect of the structural implications observed. The increased deflection values

of SHC may warrant further experiments involving hygro-thermo-chemical modeling observing the effects of loading on deformations and cracking distribution of SHC structural elements. In addition, further loading cycles may be simulated in future studies to simulate long-term performance. Aside from mechanical properties, SHC beam elements could benefit from investigating their environmental durability in exposure to different conditions in reflection of practical implications. Furthermore, simulations verified against experimental methods may improve cost quantifications and lifecycle assessments.

Author Contributions: Conceptualization, L.D.S.; methodology, K.A.; software, L.D.S.; validation, A.H.; formal analysis, L.D.S.; investigation, D.A. and R.A.; resources, L.D.S.; data curation, A.H.; writing—original draft preparation, D.A.; writing—review and editing, D.A. and R.A.; visualization, L.D.S.; supervision, L.D.S.; project administration, A.H.; funding acquisition, A.H. All authors have read and agreed to the published version of the manuscript.

Funding: This research was funded along with the APC by the Deanship of Scientific Research at Albaha University, grant number 1440/9.

Institutional Review Board Statement: Not applicable.

Informed Consent Statement: Not applicable.

Data Availability Statement: Not applicable.

Acknowledgments: The authors are grateful for the Deanship of Scientific Research at Albaha University for funding this research.

Conflicts of Interest: The authors declare no conflict of interest.

References

1. Van Belleghem, B.; van den Heede, P.; Van Tittelboom, K.; De Belie, N.D. Quantification of the Service Life Extension and Environmental Benefit of Chloride Exposed Self-Healing Concrete. *Materials* **2016**, *10*, 5. [CrossRef]
2. Van den Heede, P.; De Belie, N.; Pittau, F.; Habert, G.; Mignon, A. Life Cycle Assessment of Self-Healing Engineered Cementitious Composite (SH-ECC) Used for the Rehabilitation of Bridges. Available online: https://core.ac.uk/display/188629730 (accessed on 20 May 2022).
3. van den Heede, P.; Mignon, A.; Habert, G.; De Belie, N. Cradle-to-gate life cycle assessment of self-healing engineered cementitious composite with in-house developed (semi-)synthetic superabsorbent polymers. *Cem. Concr. Compos.* **2018**, *94*, 166–180. [CrossRef]
4. Garces, J.I.T.; Dollente, I.J.; Beltran, A.B.; Tan, R.R.; Promentilla, M.A.B. Life cycle assessment of self-healing geopolymer concrete. *Clean. Eng. Technol.* **2021**, *4*, 100147. [CrossRef]
5. Ramagiri, K.; Chintha, R.; Bandlamudi, R.; De Maeijer, P.K.; Kar, A. Cradle-to-Gate Life Cycle and Economic Assessment of Sustainable Concrete Mixes—Alkali-Activated Concrete (AAC) and Bacterial Concrete (BC). *Infrastructures* **2021**, *6*, 104. [CrossRef]
6. Li, V.C.; Herbert, E. Robust self-healing concrete for sustainable infrastructure. *J. Adv. Concr. Technology* **2012**, *10*, 207–218. [CrossRef]
7. Van Tittelboom, K.; De Belie, N. Self-Healing in Cementitious Materials—A Review. *Materials* **2013**, *6*, 2182–2217. [CrossRef]
8. Theodoridou, M.; Harbottle, M. Biological Self-Healing for the Protection of Cultural Heritage Stone Structures. Available online: https://confit.atlas.jp/guide/event-img/jpgu2018/MIS02-P05/public/pdf?type=in (accessed on 24 December 2022).
9. Vucetic, S.; Miljevic, B.; Sovljanski, O.; van der Bergh, J.M.; Markov, S.; Hirsenberger, H.; Malesevic, M.T.; Ranogajec, J. Functional mortars for conservation of cultural heritage structures. *IOP Conf. Series: Mater. Sci. Eng.* **2020**, *949*, 12091. [CrossRef]
10. Booth, P.; Jankovic, L. Novel biodesign enhancements to at-risk traditional building materials. *Front. Built Environ.* **2022**, *8*. [CrossRef]
11. Arnold, D. Self-healing concrete. *Ingenia Mag.* **2011**, *46*, 39–43.
12. Sunakh Zabanoot, M.S. Review of Autogenous and Autonomous self-Healing Concrete Technologies for Marine Environments. *High Perform. Optim. Des. Struct. Mater. IV* **2020**, *196*, 31. [CrossRef]
13. Albuhairi, D.; Di Sarno, L. Low-Carbon Self-Healing Concrete: State-of-the-Art, Challenges and Opportunities. *Buildings* **2022**, *12*, 1196. [CrossRef]
14. Yang, S.; Aldakheel, F.; Caggiano, A.; Wriggers, P.; Koenders, E. A Review on Cementitious Self-Healing and the Potential of Phase-Field Methods for Modeling Crack-Closing and Fracture Recovery. *Materials* **2020**, *13*, 5265. [CrossRef]
15. Freeman, B.L.; Bonilla-Villalba, P.; Mihai, I.C.; Alnaas, W.F.; Jefferson, A.D. A specialised finite element for simulating self-healing quasi-brittle materials. *Adv. Model. Simul. Eng. Sci.* **2020**, *7*, 32. [CrossRef]
16. Mauludin, L.M.; Zhuang, X.; Rabczuk, T. Computational modeling of fracture in encapsulation-based self-healing concrete using cohesive elements. *Compos. Struct.* **2018**, *196*, 63–75. [CrossRef]

17. Huang, H.; Ye, G. Simulation of self-healing by further hydration in cementitious materials. *Cem. Concr. Compos.* **2012**, *34*, 460–467. [CrossRef]
18. Zhelyazov, T. Numerical Simulation of the Response of Concrete Structural Elements Containing a Self-Healing Agent. *Materials* **2022**, *15*, 1233. [CrossRef]
19. Hermawan, H.; Minne, P.; Serna, P.; Gruyaert, E. Understanding the Impacts of Healing Agents on the Properties of Fresh and Hardened Self-Healing Concrete: A Review. *Processes* **2021**, *9*, 2206. [CrossRef]
20. Guzlena, S.; Sakale, G. Self-healing concrete with crystalline admixture—A review. *IOP Conf. Ser. Mater. Sci. Eng.* **2019**, *660*, 12057. [CrossRef]
21. Reddy, T.C.S.; Ravitheja, A. Macro mechanical properties of self healing concrete with crystalline admixture under different environments. *Ain Shams Eng. J.* **2019**, *10*, 23–32. [CrossRef]
22. Di Luzio, G.; Ferrara, L.; Krelani, V. Numerical modeling of mechanical regain due to self-healing in cement based composites. *Cem. Concr. Compos.* **2018**, *86*, 190–205. [CrossRef]
23. Guo, S.; Samir, C. MAT152-1 CSCE Annual Conference Growing with Youth -Croître Avec Les Jeunes Laval (Greater Montreal) Self-Healing Concrete: A Critical Review. 2019. Available online: https://www.csce.ca/elf/apps/CONFERENCEVIEWER/conferences/2019/pdfs/PaperPDFVersion_152_0423094222.pdf (accessed on 12 June 2019).
24. Gilford, J.; Hassan, M.M.; Rupnow, T.; Barbato, M.; Okeil, A.M.; Asadi, S. Dicyclopentadiene and Sodium Silicate Microencapsulation for Self-Healing of Concrete. *J. Mater. Civ. Eng.* **2014**, *26*, 886–896. [CrossRef]
25. Abaqus/Standard—Simulation of Static and Low Speed Dynamic Events. Available online: https://www.3ds.com/products-services/simulia/products/abaqus/abaqusstandard/ (accessed on 26 December 2022).
26. Öztürk, H.; Demir, A.; Caglar, N. Eurocode 2: Design of Concrete Structures | Eurocodes: Building the Future. Effect of Support Conditions on Behavior of Reinforced Concrete Short Beams. 2016. Available online: https://eurocodes.jrc.ec.europa.eu/EN-Eurocodes/eurocode-2-design-concrete-structures (accessed on 1 January 2022).
27. ACI Committee (Ed.) *Building Code Requirements for Structural Concrete (ACI318–95) and Commentary (ACI318R-95)*; American Concrete Institute: Farmington Hills, MI, USA, 1995.
28. Lubliner, J.; Oliver, J.; Oller, S.; Oñate, E. A Plastic-Damage Model for Concrete. *Int. J. Solids Struct.* **1989**, *25*, 299–326. Available online: https://www.semanticscholar.org/paper/A-plastic-damage-model-for-concrete-Lubliner-Oliver/4d383d4dc71548595d099fe7ec8513c1e0023b0d (accessed on 3 February 2023). [CrossRef]
29. Lee, J.; Fenves, G.L. Plastic-Damage Model for Cyclic Loading of Concrete Structures. *J. Eng. Mech.* **1998**, *124*, 892–900. [CrossRef]
30. Lee, S.-H.; Abolmaali, A.; Shin, K.-J.; Lee, H.-D. ABAQUS modeling for post-tensioned reinforced concrete beams. *J. Build. Eng.* **2020**, *30*, 101273. [CrossRef]
31. George, J.; Kalyana Rama, J.S.; Siva Kumar, M.V.N.; Vasan, A. Behavior of Plain Concrete Beam subjected to Three Point Bending using Concrete Damaged Plasticity (CDP) Model. *Mater. Today Proc.* **2017**, *4*, 9742–9746. [CrossRef]
32. Labibzadeh, M.; Zakeri, M.; Shoaib, A.A. A new method for CDP input parameter identification of the ABAQUS software guaranteeing uniqueness and precision. *Int. J. Struct. Integr.* **2017**, *8*, 264–284. [CrossRef]
33. Vijay, K.; Murmu, M. Self-repairing of concrete cracks by using bacteria and basalt fiber. *SN Appl. Sci.* **2019**, *1*, 1344. [CrossRef]
34. Mirshahmohammad, M.; Rahmani, H.; Maleki-Kakelar, M.; Bahari, A. Effect of sustained service loads on the self-healing and corrosion of bacterial concretes. *Constr. Build. Mater.* **2022**, *322*, 126423. [CrossRef]
35. Giannaros, P.; Kanellopoulos, A.; Al-Tabbaa, A. Sealing of cracks in cement using microencapsulated sodium silicate. *Smart Mater. Struct.* **2016**, *25*, 84005. [CrossRef]
36. Ravitheja, A.; Reddy, T.C.S.; Sashidhar, C. Self-Healing Concrete with Crystalline Admixture—A Review. *J. Wuhan Univ. Technol. Sci. Ed.* **2019**, *34*, 1143–1154. [CrossRef]

Disclaimer/Publisher's Note: The statements, opinions and data contained in all publications are solely those of the individual author(s) and contributor(s) and not of MDPI and/or the editor(s). MDPI and/or the editor(s) disclaim responsibility for any injury to people or property resulting from any ideas, methods, instructions or products referred to in the content.